



**Targeted 3' Processing of Antisense Transcripts Triggers
Arabidopsis FLC Chromatin Silencing**

Fuquan Liu, *et al.*

Science **327**, 94 (2010);

DOI: 10.1126/science.1180278

This copy is for your personal, non-commercial use only.

If you wish to distribute this article to others, you can order high-quality copies for your colleagues, clients, or customers by [clicking here](#).

Permission to republish or repurpose articles or portions of articles can be obtained by following the guidelines [here](#).

The following resources related to this article are available online at www.sciencemag.org (this information is current as of September 9, 2011):

Updated information and services, including high-resolution figures, can be found in the online version of this article at:

<http://www.sciencemag.org/content/327/5961/94.full.html>

Supporting Online Material can be found at:

<http://www.sciencemag.org/content/suppl/2009/12/08/science.1180278.DC1.html>

This article **cites 26 articles**, 11 of which can be accessed free:

<http://www.sciencemag.org/content/327/5961/94.full.html#ref-list-1>

This article has been **cited by** 1 article(s) on the ISI Web of Science

This article has been **cited by** 12 articles hosted by HighWire Press; see:

<http://www.sciencemag.org/content/327/5961/94.full.html#related-urls>

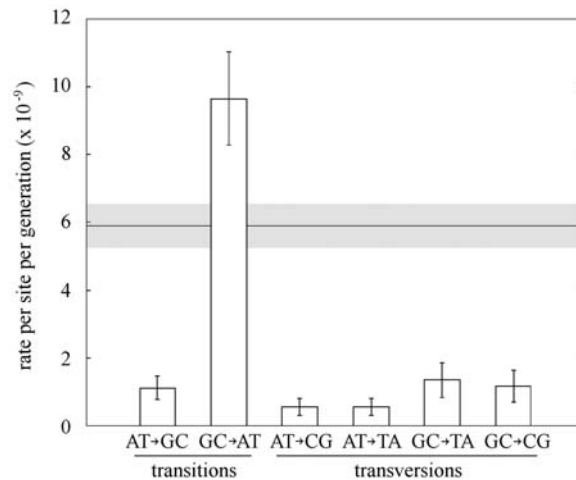
This article appears in the following **subject collections**:

Botany

<http://www.sciencemag.org/cgi/collection/botany>

Downloaded from www.sciencemag.org on September 9, 2011

Fig. 2. Conditional mutation rates per A:T or G:C site per generation. Complementary mutations, such as A→C and T→G, are pooled. Error bars indicate standard errors of the mean. The overall mutation rate, which is the average of the total mutation rates at A:T and G:C sites, and its standard error in gray are shown in the background. Only estimates from the consensus method are shown.



reported to be at least partially methylated had a higher probability of mutation to A:T than non-methylated sites (Fisher's exact test, $P = 3.2 \times 10^{-7}$). However, 91% of G:C sites in *A. thaliana* were not reported to be methylated, and they too had a higher rate of transition (but not transversion) than A:T sites (Fisher's exact test, $P = 1.2 \times 10^{-8}$). G:C sites in CpG contexts are known to be more frequently methylated (20, 21). However, transitions at G:C sites not known to be methylated do not happen in CpG contexts more often than expected by chance (Fisher's exact test, $P = 0.6$). This suggests that factors in addition to methylation contribute to the high rate of transitions at G:C sites.

In both prokaryotes and eukaryotes, most of the mutations caused by ultraviolet (UV) light are G: C→A:T transitions at sites where the C is adjacent to another C or to a T (dipyrimidine sites) (22). Among the 33 observed transition mutations at nonmethylated G:C sites, 31 were in dipyrimidine contexts, which is more than expected by chance at the $P = 0.02$ level (Fisher's exact test). Thus, we conclude that the increased rate of transitions at G:C sites, relative to A:T sites, can be largely explained by the combined effect of UV-induced mutagenesis and deamination of methylated cytosines. This implies that the mutation rate in nature could be higher than that reported here, because UV radiation during the MA experiment was probably lower than in natural conditions.

We used the *Arabidopsis* Information Resource (TAIR) 8 annotation (www.arabidopsis.org) to group all analyzed sites into the functional classes: intergenic, intronic, untranslated region (UTR), coding, pseudogene, mobile element, and non-coding. There is no deficit of nonsynonymous mutations (G test, $P = 0.4$), supporting the notion that the mutation rate we observed is not affected by selection. We did, however, observe an excess of intergenic mutations, relative to mutations in coding regions, introns, and UTRs (fig. S3). These differences were still significant after taking into account the effects of base composition and methylation (G test, $P = 0.00025$). To test whether the lack of mutations in genic regions was due to undetected levels of selection, we compared the intergenic

mutation rate with the rate at synonymous sites and introns, which are less likely to be under strong selection, and we still detected a significant deficit of mutations in the latter (Fisher's exact test, $P = 0.001$, for nonmethylated sites). We attribute the deficit of genic mutations to our observation of a higher mutation rate in pericentromeric regions (see above), where gene density is lower (5), although transcription-coupled DNA repair could also contribute to the pattern. Lastly, the finding of a higher mutation rate in pericentromeric regions provides an explanation of the *Arabidopsis*-specific pattern of higher polymorphism levels near the centromeres (16, 23), although the underlying mechanism of such a mutational bias remains to be explained.

References and Notes

1. M. Lynch *et al.*, *Proc. Natl. Acad. Sci. U.S.A.* **105**, 9272 (2008).
2. D. R. Denver *et al.*, *Proc. Natl. Acad. Sci. U.S.A.* **106**, 16310 (2009).

3. P. D. Keightley *et al.*, *Genome Res.* **19**, 1195 (2009).
4. R. G. Shaw, D. L. Byers, E. Darmo, *Genetics* **155**, 369 (2000).
5. Arabidopsis Genome Initiative, *Nature* **408**, 796 (2000).
6. S. Ossowski *et al.*, *Genome Res.* **18**, 2024 (2008).
7. K. Schneeberger *et al.*, *Genome Biol.* **10**, R98 (2009).
8. Materials and methods are available as supporting material on Science Online.
9. M. Lynch, *Mol. Biol. Evol.* **25**, 2409 (2008).
10. M. A. Quail *et al.*, *Nat. Methods* **5**, 1005 (2008).
11. T. N. Marriage *et al.*, *Heredity* **103**, 310 (2009).
12. K. H. Wolfe, W.-H. Li, P. M. Sharp, *Proc. Natl. Acad. Sci. U.S.A.* **84**, 9054 (1987).
13. S. T. Schultz, M. Lynch, J. H. Willis, *Proc. Natl. Acad. Sci. U.S.A.* **96**, 11393 (1999).
14. F. H. Shaw, C. J. Geyer, R. G. Shaw, *Evolution* **56**, 453 (2002).
15. S. I. Wright, B. Lauga, D. Charlesworth, *Mol. Biol. Evol.* **19**, 1407 (2002).
16. R. M. Clark *et al.*, *Science* **317**, 338 (2007).
17. T. Lindahl, B. Nyberg, *Biochemistry* **13**, 3405 (1974).
18. C. Coulondre, J. H. Miller, P. J. Farabaugh, W. Gilbert, *Nature* **274**, 775 (1978).
19. B. K. Duncan, J. H. Miller, *Nature* **287**, 560 (1980).
20. S. J. Cokus *et al.*, *Nature* **452**, 215 (2008).
21. R. Lister *et al.*, *Cell* **133**, 523 (2008).
22. E. C. Friedberg *et al.*, *DNA Repair and Mutagenesis* [ASM (American Society for Microbiology) Press, Washington, DC, 2006].
23. A. Kawabe, A. Forrest, S. I. Wright, D. Charlesworth, *Genetics* **179**, 985 (2008).
24. We thank C. Lanz for generating the Illumina data, S. E. Jacobsen for providing the methylation data, and P. Tiffin for valuable comments. Funded by the Deutsche Forschungsgemeinschaft (DFG) (ERA-PG ARelatives), a Gottfried Wilhelm Leibniz Award (DFG), the Max Planck Society (D.W.), NIH grant GM36827 to M. L. and W. Kelly Thomas, Pioneer Hi-Bred International to E. Darmo, and NSF grants DEB 9629457 and 9981891 to R.G.S.

Supporting Online Material

www.sciencemag.org/cgi/content/full/327/5961/92/DC1
Materials and Methods
SOM Text
Figs. S1 to S8
Tables S1 to S3
References

17 August 2009; accepted 27 October 2009
10.1126/science.1180677

Targeted 3' Processing of Antisense Transcripts Triggers *Arabidopsis FLC* Chromatin Silencing

Fuqan Liu,* Sebastian Marquardt,* Clare Lister, Szymon Swiezewski,† Caroline Dean‡

Noncoding RNA is emerging as an important regulator of gene expression in many organisms. We are characterizing RNA-mediated chromatin silencing of the *Arabidopsis* major floral repressor gene, *FLC*. Through suppressor mutagenesis, we identify a requirement for CstF64 and CstF77, two conserved RNA 3'-end-processing factors, in *FLC* silencing. However, *FLC* sense transcript 3' processing is not affected in the mutants. Instead, CstF64 and CstF77 are required for 3' processing of *FLC* antisense transcripts. A specific RNA-binding protein directs their activity to a proximal antisense polyadenylation site. This targeted processing triggers localized histone demethylase activity and results in reduced *FLC* sense transcription. Targeted 3' processing of antisense transcripts may be a common mechanism triggering transcriptional silencing of the corresponding sense gene.

Extensive noncoding RNA has been found in many organisms (1, 2). The degree and mechanism of processing of these transcripts is unclear, as studies of RNA processing

have so far focused on coding (messenger) RNA transcripts in mammalian and yeast cells. The large protein complex mediating 3'-end processing and polyadenylation has recently been de-

scribed (3, 4); however, its role in processing noncoding transcripts is unknown. Analysis of 3' processing of unstable noncoding RNAs has identified independent termination pathways with different components (5).

We have been studying the function of RNA processing in chromatin regulation through analysis of the gene encoding the major *Arabidopsis* floral repressor FLOWERING LOCUS C (*FLC*) (6). The autonomous floral promotion pathway results in *FLC* transcriptional silencing through the activities of two RNA-binding proteins, FCA and FPA; a member of a cleavage and polyadenylation specificity factor (CPSF) RNA 3'-processing complex, FY, which interacts directly with FCA (7, 8); and FLD, a dimethylated histone H3 at lysine 4 (H3K4me2) demethylase and homolog of human LSD1 (9).

To better understand how RNA 3'-processing links to histone modification to result in *FLC* silencing, we sought to identify all the components necessary for FCA-mediated *FLC* repression through suppressor mutagenesis. We generated an *Arabidopsis* line sensitized to FCA action expressing *35S::FCA γ* —a transgene overexpressing FCA, *FRIGIDA*—a strong activator of *FLC* expression and *FLC::LUC*, so *FLC* expression could be monitored with a bioluminescence detection assay (10, 11). Mutations that suppressed the ability of FCA to repress *FLC*, together with an epistasis analysis of their interaction with *fca* mutants, enabled us to identify components required for FCA action (fig. S1). These mutations, named suppressors of overexpressed FCA (*sof*) (9), identified additional alleles of known FCA pathway components *FY* and *FLD* (fig. S2) and new complementation groups *sof2* and *sof19* (Fig. 1A and fig. S2). Genetic mapping and sequencing revealed *sof2* and *sof19* carried mutations in *CstF77* (At1g17760) and *CstF64* (At1g71800), respectively (fig. S3, A to C).

CstF77 and *CstF64* are the *Arabidopsis* homologs of two of the three components of the CstF RNA 3'-processing complex, conserved from yeast to plants and humans (12). *CstF77* is a single-copy gene in the *Arabidopsis* genome. In *sof2* (carrying the *cstf77-1* allele), the splice acceptor site in intron 12 is mutated, which leads to an in-frame deletion of Tyr³³⁹ to Lys³⁸⁵ in exon 13 (fig. S3A). *CstF77* is an essential gene in other organisms (13, 14), yet *cstf77-1* plants are viable, but their flowering is delayed. *cstf77-1* is likely to be a hypomorphic allele, because homozygous mutant progeny could not be identified from a mutation caused by a transferred DNA insertion into the 5' end of the gene (*cstf77-2*) (fig. S3A). Further analysis suggested that *cstf77-2* causes female gametophytic lethality (fig. S4, A and B),

consistent with an essential function for *CstF77*. The *sof19* mutation introduces a premature stop codon in the only full-length homolog of *CstF64* in the *Arabidopsis* genome (fig. S3A). This allele (*cstf64-1*) also reduces fertility of the plants. A second, strong allele in Columbia (Col) background (*cstf64-2*) (fig. S3A) leads to reduced organ size, pale leaves, and sterility (fig. S4, C to E). Therefore, *CstF64* function is generally required in plant growth and development. In mammals, *CstF77* interacts physically with *CstF64* through a proline-rich region (15). This interaction was found to be conserved in plants and to be unaffected by the in-frame deletion in *cstf77-1* (fig. S4F).

We further analyzed the involvement of *CstF64* and *CstF77* in *FLC* repression in genotypes not sensitized to FCA action. *cstf64-1*, *cstf64-2*, and *cstf77-1* had elevated *FLC* mRNA levels and flowered later than their respective controls (Fig. 1, B and C, and fig. S5). We also undertook an epistasis analysis to determine whether the CstF components functioned in the same pathway with known FCA pathway components, namely FCA, FY, and FLD. *cstf64-2* was not additive with *fca-9*, *fy-2*, or *fld-4* mutations but was additive with *fve-3* on the basis of analysis of both flowering time and *FLC* expression levels (Fig. 1C and fig. S6). FVE functions to repress *FLC* expression by histone deacetylation in an FCA-independent manner (16). In summary, our analysis demonstrates that CstF components do function in the same pathway as FCA in the repression of *FLC*.

Because the genetic analysis established that CstF components function with the histone demethylase FLD to down-regulate *FLC*, we tested whether the increased *FLC* in *cstf* mutants was an effect of defective transcriptional repression. *cstf64* and *cstf77* mutants showed elevated *FLC* nascent transcript levels (Fig. 2B and fig. S7);

higher RNA polymerase II (Pol II) association at *FLC* (Fig. 2C); and higher levels of H3K4me3, a histone modification associated with active transcription (17) (Fig. 2D). The CstF complex is generally required for canonical mRNA 3'-end formation (12), but its loss did not affect *FLC* sense RNA 3' processing; indeed, *FLC* sense levels accumulate and are functional as evidenced by the late flowering of *cstf64* double mutants (Fig. 1C). Thus, CstF components mediate transcriptional repression of *FLC* levels but are unlikely to be required for *FLC* mRNA 3'-end formation.

FCA directly associates with *FLC* chromatin (9), so one explanation for our observations is that the substrates of *CstF64*, *CstF77*, FCA, and FY are other nascent transcripts from the *FLC* locus. We have previously described alternatively polyadenylated *FLC* antisense transcripts (9, 18). One polyadenylation site of the *FLC* antisense RNA coincides with the location of FCA on *FLC* chromatin, whereas a distal polyadenylation site overlaps with the *FLC* sense promoter (9). Quantitative reverse transcription polymerase chain reaction (qRT-PCR) analysis revealed increased levels of *FLC* antisense transcription in *fca*, *fy*, and *cstf* mutants (fig. S8A). Further analysis has also revealed additional complexity in the antisense transcripts, so we developed an assay to detect RNA 3' processing and polyadenylation at the specific polyadenylation sites shown in Fig. 3. qRT-PCR revealed that *FLC* antisense RNA 3' processing was reduced at both proximal and distal polyadenylation sites in *cstf64* and *cstf77* (Fig. 3B), but *FLC* sense RNA polyadenylation was not reduced (fig. S8B). Thus, 3' processing and polyadenylation of *FLC* antisense transcripts, but not *FLC* sense transcripts, appear sensitive to CstF complex activity. Rapid amplification of cDNA 3' ends (RACE) analysis revealed that the same polyadenylation sites are

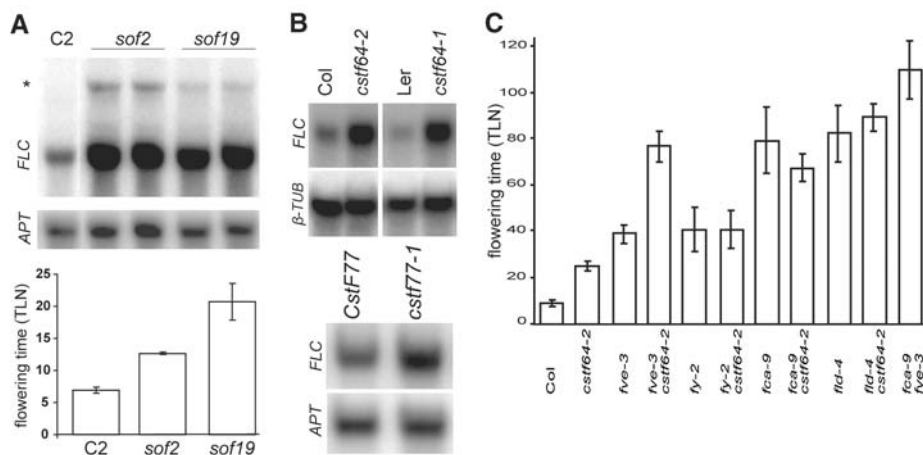


Fig. 1. CstF64 and CstF77 regulate *FLC* levels. (A) Northern and flowering time analysis (total leaf number) of *sof2* (*cstf77-1* in FCA-sensitized background) and *sof19* (*cstf64-1* in FCA-sensitized background). Asterisk indicates *FLC::LUC*; APT is the loading control. (B) Northern analysis of *FLC* levels in *cstf64* carrying no transgenes or *cstf77* carrying the linked *FRI* transgene. β -TUB or APT is the loading control. (C) *cstf64-2* is not additive with *fca-9*, *fy-2*, or *fld-4* (all Col genotype). (A) and (C) graph values are means \pm SD ($n = 20$).

Department of Cell and Developmental Biology, John Innes Centre, Norwich NR4 7UH, UK.

*These authors contributed equally to this work.

†Present address: Institute of Biochemistry and Biophysics, Polish Academy of Sciences, 02-106 Warsaw, Poland.

‡To whom correspondence should be addressed. E-mail: caroline.dean@bbsrc.ac.uk

used in the *fca* mutant and wild type; however, qRT-PCR, supported by strand-specific Northern analysis, showed that the relative usage of each site differed. In *fca* and *fy*, proximal site usage was reduced, and in *fca*, distal site usage increased (Fig. 3C and fig. S8C). This is not a feature of general *FLC* de-repression, because

proximal site usage was not affected in *five* (Fig. 3C) (16). To investigate the generality of this finding, we analyzed the effects of FPA, a second RNA recognition motif (RRM) protein that functions in the autonomous floral promotion pathway. FPA also requires FLD to repress *FLC* (19), but it functions independently of FCA (19). As

in *fca*, proximal site usage in the *FLC* antisense transcript was reduced, and distal site usage increased in *fpa-7* (Fig. 3C). Because the two RRM proteins trigger *FLC* silencing independently, we predicted that disruption of FPA function would cause increased *FLC* expression even in the sensitized FCA background. This was confirmed through the identification of *sof34* as a novel *fpa* mutation (fig. S9). Taken together, these results reveal that both RNA-binding proteins independently function to promote 3' processing at the proximal site in the *FLC* antisense transcript and that this activity triggers *FLC* sense strand transcriptional silencing.

The position of the proximal 3'-processing site on the antisense transcript coincides with the site where FCA associates with *FLC* chromatin (9). This suggests a model whereby FCA, interacting with a component of the CPSF complex, targets CstF-dependent 3' processing to the proximal site on *FLC* antisense transcripts (fig. S10). An indirect effect, via CstF regulation of an intermediary regulator, is possible, but unlikely, because of the direct association of FCA with *FLC*. Proximal *FLC* antisense transcript 3' processing is promoted by FCA and FY (Fig. 3), which is reminiscent of the FCA-FY interaction-dependent 3'-processing site choice in *FCA* negative-feedback regulation (7). FPA also enhances usage of this proximal 3'-processing site. These activities then appear to converge to trigger FLD-dependent demethylation of H3K4me2 in the body of the gene, downstream of the proximal polyadenylation site. We speculate that this may involve termination-associated processes, perhaps cotranscriptional decay of the antisense RNA downstream of the cleavage site (20). Whatever the mechanism, down-regulation of both sense and antisense transcription is the net result. We suspect the activity of DICER-LIKE3, previously shown to function in this process (9), is required to couple the 3' processing to FLD histone demethylase function (21); however, RNA polymerases involved in silencing mediated by small interfering RNA (siRNA) (18) only weakly suppress FCA activity (fig. S11). A role for small RNAs in the targeting of the histone demethylase activity to the central part of the locus may lead to *trans* effects on homologous sequences in the genome, perhaps explaining the small effect of an *fca* mutation on an *FLC* transgene lacking the 3' region (22).

The proteins involved in this silencing mechanism—two RRM proteins, a factor associated with 3' processing components, and a conserved histone demethylase—also silence transposons and transgenes in *Arabidopsis* (20, 23). This mechanism may therefore play a more general role, rather than only regulating the floral repressor gene, *FLC*. This is consistent with the role for CPSF complex components in suppressing viral amplicon-induced gene silencing in *Arabidopsis* (24). This mechanism may also be very important in nonplant genomes. Genome-wide antisense transcripts, identified in

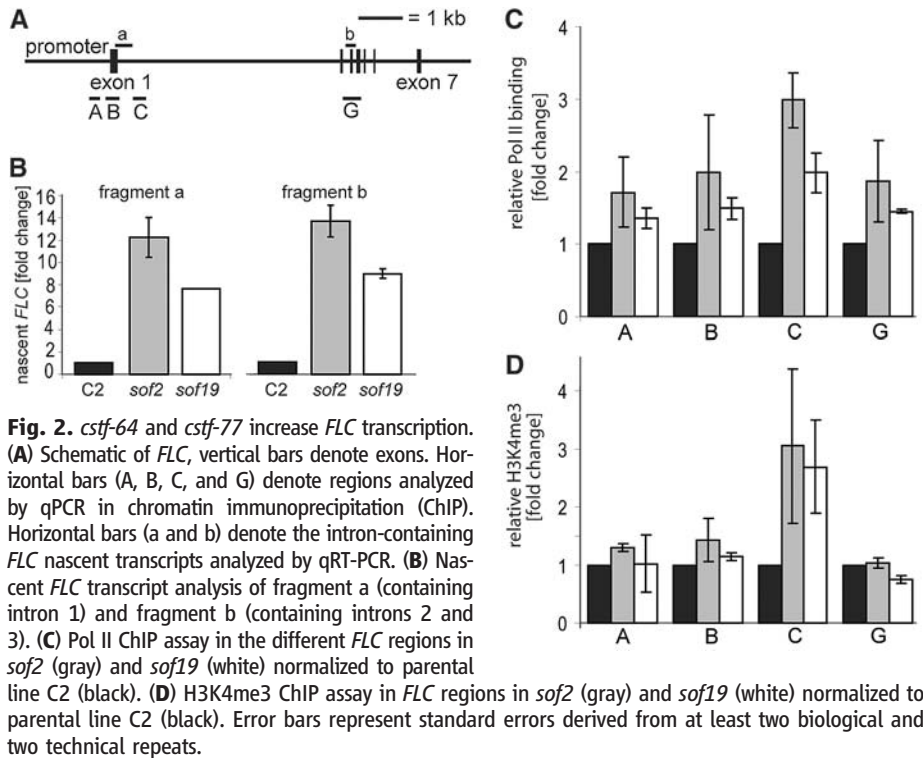


Fig. 2. *cstf-64* and *cstf-77* increase *FLC* transcription. (A) Schematic of *FLC*, vertical bars denote exons. Horizontal bars (A, B, C, and G) denote regions analyzed by qPCR in chromatin immunoprecipitation (ChIP). Horizontal bars (a and b) denote the intron-containing *FLC* nascent transcripts analyzed by qRT-PCR. (B) Nascent *FLC* transcript analysis of fragment a (containing intron 1) and fragment b (containing introns 2 and 3). (C) Pol II ChIP assay in the different *FLC* regions in *sof2* (gray) and *sof19* (white) normalized to parental line C2 (black). (D) H3K4me3 ChIP assay in *FLC* regions in *sof2* (gray) and *sof19* (white) normalized to parental line C2 (black). Error bars represent standard errors derived from at least two biological and two technical repeats.

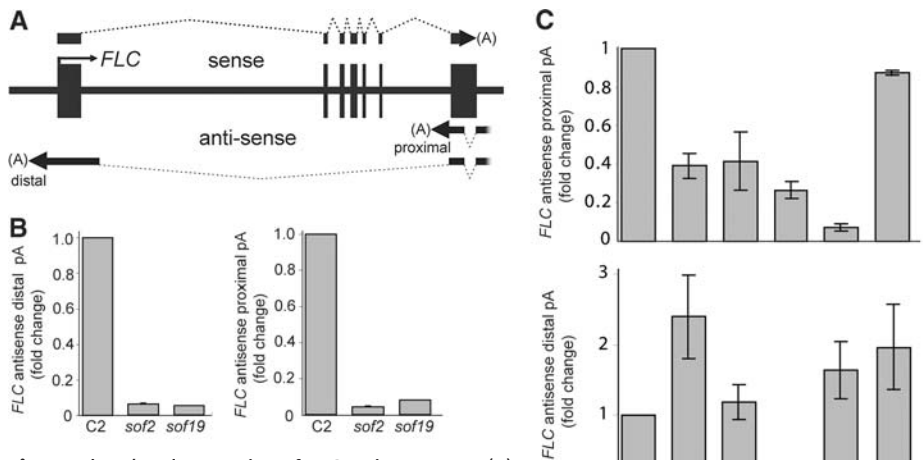


Fig. 3. The 3' end processing of *FLC* antisense RNA. (A) In this *FLC* schematic, vertical bars denote exons; transcription start site of *FLC* sense RNA is indicated by an arrow. *FLC* sense (top) and antisense (bottom) transcripts with dashed lines indicating introns, arrows with symbol (A) are polyadenylation sites, and shading shows the region of multiple antisense RNA start sites. (B) The 3' processing of *FLC* antisense transcripts is reduced at both distal and proximal sites in *sof2* and *sof19*. *FLC* antisense transcript levels are normalized to total *FLC* antisense transcript and given as fold change compared with the parental line C2. (C) The 3' processing of *FLC* antisense transcripts at the proximal (top) and the distal sites (bottom) in different mutants (all in the Col genotype without transgene). *FLC* antisense transcript levels are normalized to total *FLC* antisense transcript and given as fold change compared with the Col wild type. The raw qPCR data are given in table S1. In (B) and (C), averages and standard errors of three biological repeats with two technical repeats are shown.

many organisms, function in chromatin silencing (2, 25, 26) and RNA 3'-processing components mediate gene silencing in *Caenorhabditis elegans* (27). Therefore, the 3' processing of antisense transcripts may be a general mechanism triggering chromatin silencing in eukaryotes.

References and Notes

- B. T. Wilhelm *et al.*, *Nature* **453**, 1239 (2008).
- C. P. Ponting, P. L. Oliver, W. Reik, *Cell* **136**, 629 (2009).
- M. J. Moore, N. J. Proudfoot, *Cell* **136**, 688 (2009).
- Y. Shi *et al.*, *Mol. Cell* **33**, 365 (2009).
- L. Vasiljeva, M. Kim, N. Terzi, L. M. Soares, S. Buratowski, *Mol. Cell* **29**, 313 (2008).
- G. G. Simpson, *Curr. Opin. Plant Biol.* **7**, 570 (2004).
- G. G. Simpson, P. P. Dijkwel, V. Quesada, I. Henderson, C. Dean, *Cell* **113**, 777 (2003).
- D. Manzano *et al.*, *Proc. Natl. Acad. Sci. U.S.A.* **106**, 8772 (2009).
- F. Liu *et al.*, *Mol. Cell* **28**, 398 (2007).
- J. Mylne, T. Greb, C. Lister, C. Dean, *Cold Spring Harb. Symp. Quant. Biol.* **69**, 457 (2004).
- Materials and methods are available as supporting material on Science Online.
- J. Zhao, L. Hyman, C. Moore, *Microbiol. Mol. Biol. Rev.* **63**, 405 (1999).
- M. Simonelig, K. Elliott, A. Mitchelson, K. O'Hare, *Genetics* **142**, 1225 (1996).
- L. Minvielle-Sebastia, B. Winsor, N. Bonneaud, F. Lacroute, *Mol. Cell. Biol.* **11**, 3075 (1991).
- Y. Bai *et al.*, *Mol. Cell* **25**, 863 (2007).
- I. Ausin, C. Alonso-Blanco, J. A. Jarillo, L. Ruiz-Garcia, J. M. Martinez-Zapater, *Nat. Genet.* **36**, 162 (2004).
- B. Li, M. Carey, J. L. Workman, *Cell* **128**, 707 (2007).
- S. Swiezewski *et al.*, *Proc. Natl. Acad. Sci. U.S.A.* **104**, 3633 (2007).
- I. Baurle, C. Dean, *PLoS One* **3**, e2733 (2008).
- M. Kim *et al.*, *Nature* **432**, 517 (2004).
- T. Iida, J.-i. Nakayama, D. Moazed, *Mol. Cell* **31**, 178 (2008).
- C. C. Sheldon, A. B. Conn, E. S. Dennis, W. J. Peacock, *Plant Cell* **14**, 2527 (2002).
- I. Baurle, L. Smith, D. C. Baulcombe, C. Dean, *Science* **318**, 109 (2007).
- A. J. Herr, A. Molnar, A. Jones, D. C. Baulcombe, *Proc. Natl. Acad. Sci. U.S.A.* **103**, 14994 (2006).
- J. Camblong, N. Iglesias, C. Fickentscher, G. Dieppois, F. Stutz, *Cell* **131**, 706 (2007).
- T. A. Volpe *et al.*, *Science* **297**, 1833 (2002).
- J. K. Kim *et al.*, *Science* **308**, 1164 (2005).
- We thank our colleagues for comments and advice and G. Szitty for comments on the manuscript. Supported by a UK Biotechnology and Biological Sciences Research Council (BBSRC) Core Strategic grant to John Innes Centre; BBSRC grant BB/D010799/1 (C.D.); European Union (EU) Marie Curie studentship MEST-CT-2005-019727 to S.M.; EU Framework VI program Integrated Project LSHG-CT-2006-037900.

Supporting Online Material

www.sciencemag.org/cgi/content/full/1180278/DC1

Materials and Methods

SOM Text

Figs. S1 to S11

Table S1

References

7 August 2009; accepted 27 October 2009

Published online 3 December 2009;

10.1126/science.1180278

Include this information when citing this paper.

Reproducibility Distinguishes Conscious from Nonconscious Neural Representations

Aaron Schurger,^{1,2*} Francisco Pereira,^{1,2} Anne Treisman,¹ Jonathan D. Cohen^{1,2}

What qualifies a neural representation for a role in subjective experience? Previous evidence suggests that the duration and intensity of the neural response to a sensory stimulus are factors. We introduce another attribute—the reproducibility of a pattern of neural activity across different episodes—that predicts specific and measurable differences between conscious and nonconscious neural representations independently of duration and intensity. We found that conscious neural activation patterns are relatively reproducible when compared with nonconscious neural activation patterns corresponding to the same perceptual content. This is not adequately explained by a difference in signal-to-noise ratio.

Though once controversial, it is now widely accepted that sensory-perceptual information can be processed by the brain, even at the semantic level, without that information “reaching” or “entering” awareness (1–3). But what does it mean for neural information to reach awareness? Once the information has been encoded in neural activity, what else has to happen for it to become part of one’s subjective reality? A growing body of evidence suggests that the intensity of activation in areas that encode the contents of perception (such as the ventral-temporal cortex) is one determinant of whether or not that information contributes directly to subjective experience (4–7). However, local enhancement of a cortical sensory signal is also associated with attention (8), which can be independent of awareness (9–11). Therefore, there may be additional features other than the intensity of neural activity that distinguish conscious from nonconscious neural information.

Kinsbourne (12) proposes three interacting properties that collectively determine whether or not a neural representation will contribute directly to subjective experience: (i) the duration and (ii) the intensity of a pattern of activity and (iii) the coherence of that pattern of activity with the dominant “configuration” of neural activity at the global level. Here, we propose that another attribute of neural activity patterns, reproducibility, characterizes conscious representations. We define reproducibility as the similarity of patterns of neural activity across different instances of the same percept. We focused specifically on reproducibility because it is measurable and therefore empirically testable. A corollary of our proposal that conscious representations are more reproducible is that unconscious representations are more variable, even as they may carry information within a given episode.

We used functional magnetic resonance imaging (fMRI) to measure brain activity while subjects performed a simple visual category-discrimination task ($n = 12$ subjects) (13). Stimuli were simple line drawings of faces and houses (12 of each), rendered in two opposing but isoluminant colors (Fig. 1) (13). Visibility of

the stimuli was manipulated by using dichoptic color masking (DCM) (Fig. 1) (7). Subjects were asked to identify the category of the stimulus (face or house) on each trial, guessing if necessary, and to wager (“high” or “low” for monetary rewards) on the accuracy of each of their perceptual decisions (14–16). Wagering was used as a collateral index of subjects’ awareness of the object.

For visible stimuli, performance was at or near 100% correct for all 12 subjects, and all wagers were high. For invisible stimuli, task performance was only marginally different from chance ($54 \pm 2.5_{\text{[SEM]}}\%$ correct; $P < 0.06$, one-tailed t test), and sensitivity of high wagers to correct responses [wagering d' -prime, or d' (13)] was not different from zero (mean $d' = 0.015 \pm 0.11_{\text{[SEM]}}$; $P = 0.45$, one-tailed t test). For invisible stimuli, wagering d' and overall willingness to place high wagers were not significantly correlated across subjects [correlation coefficient (r) = 0.33, $P > 0.30$, $n = 12$ subjects]. This reassures against the possibility that wagering d' was artificially low because of an interaction with a wagering bias (16). The proportion of high wagers (for invisible stimuli) was similar for faces and houses (0.20 and 0.19, respectively).

Subjects were always aware of a visual event—a yellowish flickering square—and this provoked substantial activation in and of itself. What varied was subjects’ awareness of an object embedded in the square. We used multivariate pattern analysis to ascertain how the encoding of perceptual information differs depending on whether or not that information is present in subjective experience (17). Thus, in our analyses we focused specifically on the patterns of activation corresponding to the perceptual information of which the subject was or was not aware: the category of the object.

To verify the neural representation of category-specific information for both visible and invisible stimuli, we attempted to discriminate the category of the stimulus (faces versus houses) on the basis of the spatial pattern of neural activity in the temporal lobes [derived statistically from each run of

¹Department of Psychology, Princeton University, Princeton, NJ 08540, USA. ²Center for the Study of Brain, Mind, and Behavior, Princeton University, Princeton, NJ 08540, USA.

*To whom correspondence should be addressed. E-mail: schurger@princeton.edu